

Radio Frequency Interference Mitigation for the Spectral Observations of FAST

Chuan-Peng Zhang^{1,2}, Jie Wang¹, Jin-Long Xu^{1,2}, Peng Jiang^{1,2}

¹ National Astronomical Observatories, Chinese Academy of Sciences, 100101 Beijing, China; cpzhang@nao.cas.cn

² CAS Key Laboratory of FAST, NAOC, Chinese Academy of Sciences, 100101 Beijing, China

Abstract In radio astronomy, radio frequency interference (RFI) becomes more and more serious for radio observational facilities. The RFI always influences the searching and analysis of the interesting astronomical objects. Mitigating the RFI becomes an essential procedure in pulsar survey data processing. Five-hundred-meter Aperture Spherical radio Telescope (FAST) is an extremely sensitive radio telescope. It is necessary to find out an effective and precise RFI mitigation method for FAST data processing. In this work, we introduce a method to mitigate the RFI in FAST spectral observation as follows. Firstly, according to the characteristics of FAST spectra, we propose to use the ArPLS algorithm for baseline fitting. The test results show that it has a good performance. Secondly, we flag the RFI with four strategies, which are to flag extremely strong RFI, flag long-lasting RFI, flag polarized RFI, and flag beam-combined RFI, respectively. The test results show that all the RFI above a preset threshold could be removed. Thirdly, we make a statistics for the probabilities of polarized XX and YY RFI in FAST observations. The statistical results could tell us which frequencies are relatively quiescent. With such statistical data, we try to avoid using such frequencies in our spectral observations.

Key words: radio telescope: FAST — radio frequency interference — method — mitigation

1 INTRODUCTION

In radio astronomy, radio frequency interference (RFI) becomes more and more serious for radio observational facilities (Kesteven, 2005; An et al., 2017; Zeng et al., 2021). The days of interference-free observations in radio astronomy are long gone. Substantial pressures are coming from commercial, defense, and other interests for greater access to the radio-frequency spectrum. This means that radio astronomers can no longer rely on the regulatory authorities for an environment free from interference, and must look seriously at mitigation strategies (Fridman & Baan, 2001; Boonstra, 2005; Baan, 2011).

Mitigating the RFI becomes an essential procedure in pulsar survey and other data processing. RFI can occur in impulse type bursts persistently, variable in time or in a transient manner. The RFI properties in the integrated post-correlated data can be studied in terms of their morphology, consisting of broadband, narrow band roughly horizontal and vertical envelopes, mainly caused by the earlier described terrestrial sources, and blob RFI, which is a short, small-bandwidth signal from unknown sources (An et al., 2017; Zeng et al., 2021). The RFI amplitudes are typically much higher than the underlying astronomical signal and random noise, but some weak RFI signals are almost identical to the intensity of real celestial signals, such as pulsars and molecular spectra (An et al., 2017; Zhang et al., 2020). This will easily lead to misidentification and seriously influence the searching and analysis of

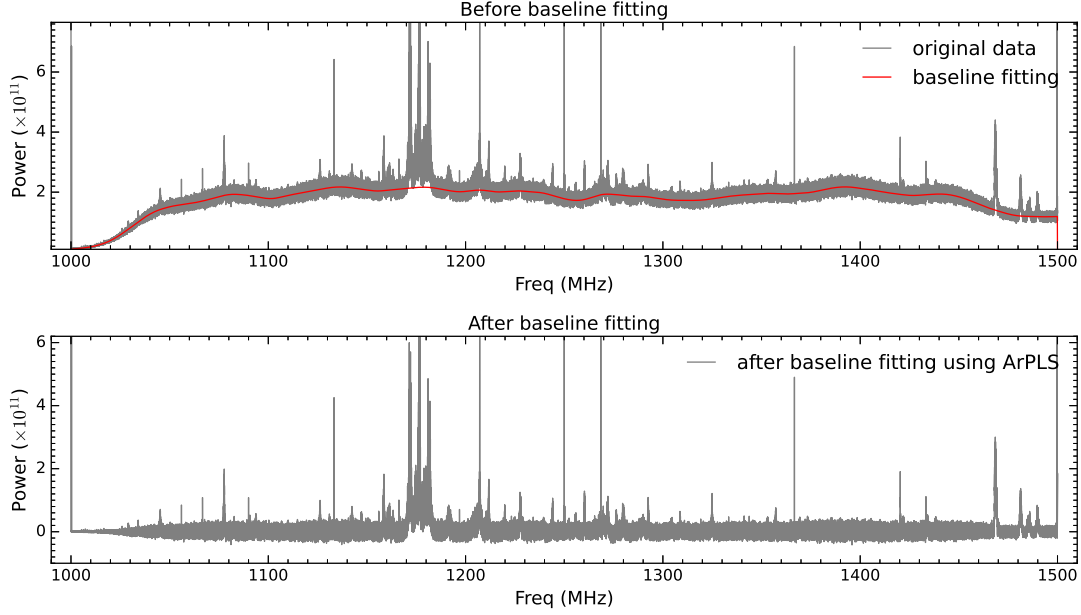


Fig. 1 A full wideband of FAST spectrum (integration time: 1 second) covering a frequency range from 1000 to 1500 MHz. All the visible emission lines except HI at 1420 MHz are RFI from terrestrial sources. The upper and lower panels show a FAST spectrum before and after baseline fitting, respectively.

the interesting astronomical objects. An important distinguishing feature for the separation of terrestrial sources of RFI from the astronomical signal relates to the amount of dispersion in the “time-frequency” domain of the received data (An et al., 2017).

FAST is located at a site position of the protected radio quiet zone in Guizhou of China. However, some strong RFI from for example, broadcast radio and TV, communication satellites and navigation satellites are extremely hard to be shielded. In addition, FAST is very susceptible to RFI from the electronic instruments integrated with the telescope and active radio services around the FAST site, due to its high sensitivity (Zhang et al., 2020). Therefore, we must look for another strategies to mitigate the RFI in FAST observations.

The aim of this work is to flag and mitigate the RFI from the FAST observations, and then give a probability and statistics for the FAST RFI showing up. Section 2 introduces the features of astronomical emission lines and terrestrial RFI in FAST observations. Section 3 presents our proposed scheme for RFI mitigation in FAST spectral observations. Section 4 shows the RFI statistical results using our proposed strategy. Section 5 gives a summary.

2 ASTRONOMICAL EMISSION LINES AND TERRESTRIAL RFI IN FAST

2.1 The characteristics for the spectral data

FAST has a 19-beam receiver for simultaneously covering multiple observational areas, thus it is a good tool to carry out drift scan observations for searching for extra-galactic point sources. The data are recorded in the spectral-line backend using a dual linear polarization (XX and YY) mode with a relatively high time-resolution. The full wideband (500 MHz) in the spectral-line backend has a frequency coverage from 1000 to 1500 MHz (see Figure 1). The high and low frequency resolution modes have

a number of 1 M and 64 K channels, respectively. The frequency resolution for the high and low resolution modes is 476.84 Hz and 7.63 KHz, respectively. The sampling time is 1 second for each spectral line. Generally, 128 seconds observation spectra are packaged into a data cube that has a size of around 2.1 GB. The aperture of the FAST is 500 m and the effective aperture is about 300 m corresponding to an HPBW of $2.9'$ at 1.4 GHz (Nan et al., 2011; Jiang et al., 2019, 2020; Han et al., 2021).

In Figure 1, we present a FAST 500 MHz spectrum with 10 seconds integration. Each spectrum in the mode of high frequency resolution has 10^6 channels in total. This leads to that the computing resources are time-consuming in reducing the FAST spectral data. We could firstly choose one out of every 400 channels, and then fit the baseline only for the selected channels. Finally, we could use interpolation technique to promote and estimate the baseline for the whole 10^6 channels.

2.2 The general RFI distribution

Figure 1 shows a full wideband of FAST spectrum covering a frequency range from 1000 to 1500 MHz. All the visible emission lines except H I at 1420 MHz are RFI that comes from terrestrial sources. The RFI, including broadcast radio and TV, cell phones, communication satellites, navigation satellites, as well as all the wireless control and monitoring systems (Zhang et al., 2020), have the potential to affect radio-astronomical observations. The RFI pollution makes the background against what radio astronomers concern be no longer dark (Boonstra, 2005).

3 THE PROPOSED SCHEME FOR RFI MITIGATION

A number of RFI mitigation methods (e.g., Fridman & Baan, 2001; Ford & Buch, 2014; Baek et al., 2015; Zhang et al., 2021b) could be used at different stages in the data acquisition process. After collecting astronomical data, however, the only thing that astronomers can do for RFI Mitigation is to flag and eliminate the effects of known and unknown sources of RFI. In the FAST astronomical spectral data, flagging RFI is seriously affected by the baseline distribution, due to that the baseline is not flat enough. Therefore, we have to firstly choose an efficient method, which is the ArPLS-based method (Baek et al., 2015), to remove the baseline, and then we could flag different types of RFI by experientially setting a credible threshold for a spectrum.

3.1 The ArPLS for baseline correction

For FAST spectrum data, We propose a baseline fitting method based on an Asymmetrically Reweighted Penalized Least Squares algorithm (ArPLS; Baek et al., 2015). The baseline correction methods based on penalized least squares have been successfully applied to various spectral analysis (e.g., Zeng et al., 2021; Zhang et al., 2021a). The methods could change a parameter “weight” iteratively to estimate a baseline. If a signal is below a previously fitted baseline, large weight is given. On the other hand, no weight or small weight is given when a signal is above a fitted baseline as it could be assumed to be a part of spectral peak. A preset coefficient λ will control the balance between fitness and smoothness (see FAST spectrum with baseline correction in Figure 1). We experientially set it to 10^5 , a constant, which could obtain satisfactory results for all of the available FAST data. This method could estimate the noise level iteratively and adjust the weights correspondingly (Baek et al., 2015).

The penalized constraint in this method makes the baseline fitting more robust and accurate than traditional methods by mitigating the negative influences from instrumental response (Baek et al., 2015). After removing the estimated baseline based on the ArPLS (see Figure 1), several novel strategies were proposed for flagging different types of RFI (see Section 3.2).

3.2 Flag different types of RFI

The RFI-flagging method mentioned above mainly targets at the FAST drift scan observations for searching for extra-galactic point sources. In this work, the used test data is the drift scan survey to-

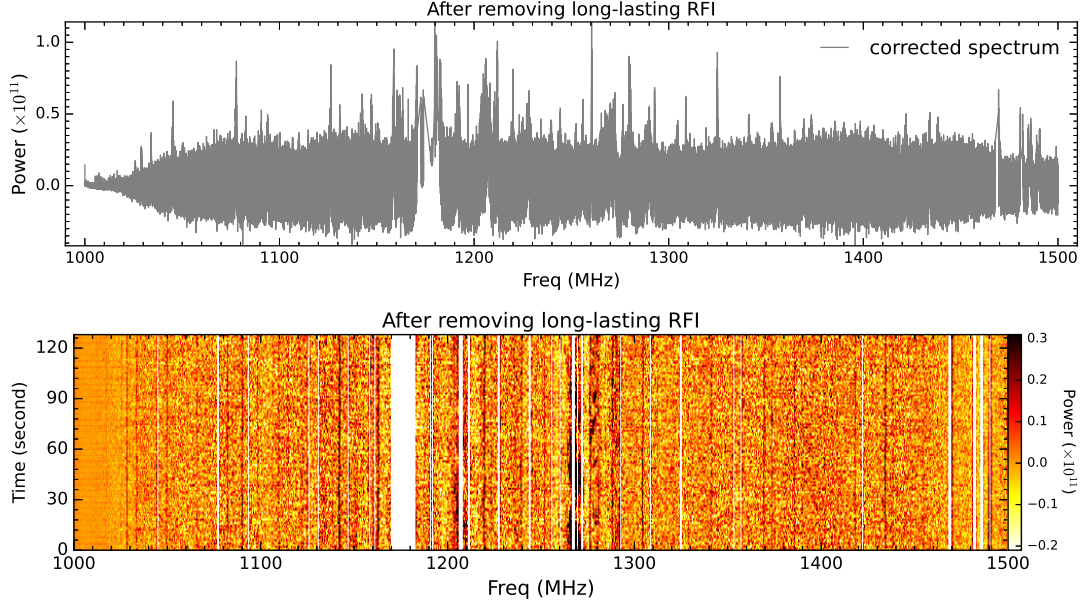


Fig. 2 Upper: A FAST spectrum (integration time: 1 second) after removing long-lasting (128 seconds) RFI above a threshold of 4σ . Lower: A 128 seconds waterfall image after removing long-lasting RFI.

wards the M31 region¹. The project number is 3047 and the observation date is between 2019 and 2020. This project will blindly map a region of 700 square degrees towards the M31 and its dark matter halo in L band with about 700 FAST hours. Based on the characteristics of the RFI in FAST after baseline correction, we adopt several strategies to flag them as follows.

3.2.1 Flag extremely strong RFI

In FAST observations, there indeed exist many extremely strong and evident RFI, for example those from communication satellites and navigation satellites at around 1175, 1207, 1270, and 1480 MHz (see the emission line in Fig. 1). These strong RFI have a serious effect on the FAST data reduction. These RFI could be easily removed by setting a reasonable threshold ($> 3\sigma$) in the baseline fitted spectrum. For example, we could remove the spectral channels above power = 2×10^{11} (see the lower panel of Figure 1). However, if we could not make sure whether they are RFI, we could skip this step.

3.2.2 Flag long-lasting RFI

In the FAST drift scan survey, generally these long-lasting (e.g., 128 seconds) emission should be RFI except the H I line at around 1.4 GHz. The reason is that almost all the extragalactic galaxies are close to point source relatively to the beam size of FAST, leading to that the signals cannot be lasting for long times. Therefore, we could firstly average some spectra (e.g., averaging 6 seconds spectra in this test work) that are close in time sequence (aim to improve signal-to-noise ratio), and then set a reasonable threshold to remove this kind of RFI (see Figure 2). Those still existing strong emission (power $> 0.5 \times 10^{11}$; see Figure 3) cannot be lasting in 128 seconds, thus they are not flagged as such kind of RFI.

¹ <https://fastwww.china-vo.org/cms/article/23/>

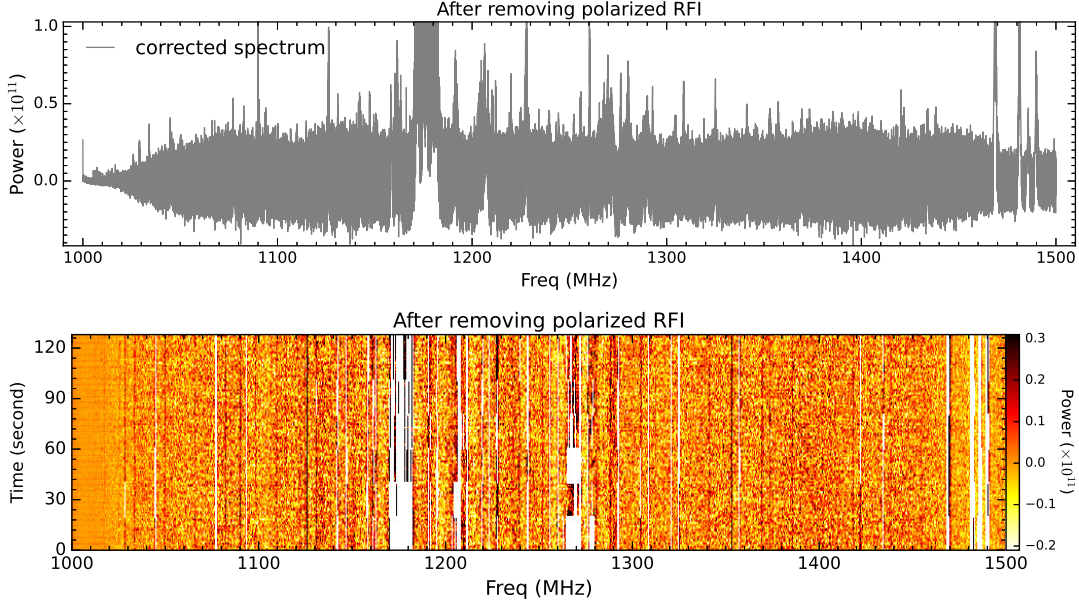


Fig. 3 Upper: A FAST spectrum (integration time: 1 second) after removing polarized (128 seconds) RFI above a threshold of 4σ . Lower: A 128 seconds waterfall image after removing polarized RFI.

3.2.3 Flag polarized RFI

For FAST observation, a dual polarization receiver is equipped in the backend, thus we could get two different polarized (XX and YY) emission simultaneously (Jiang et al., 2019, 2020). A key fact is that the signals from the extragalactic galaxies are almost non-polarized, but most of the terrestrial RFI are polarized. Therefore, we could firstly average some spectra (e.g., averaging 6 seconds spectra in this test work) that are close in time sequence (aim to improve signal-to-noise ratio). With their discrepancy, we then set a reasonable threshold to flag those polarized RFI from the terrestrial (see Figure 3). Those still existing strong emission (power $> 1 \times 10^{11}$; see Figure 3) after this setup are non-polarized RFI.

3.2.4 Flag beam-combined RFI

The FAST has a powerful 19-beam receiver, which could simultaneously cover 19 different beam-size areas (Jiang et al., 2019, 2020). In FAST drift scan survey, almost all the distant extragalactic galaxies are close to point source relatively to the beam size of FAST. This leads to that the true extragalactic signals could not simultaneously go into any two of the 19-beam receiver in a high probability. However, the observed terrestrial RFI by all the 19 receivers should get the same emission. We could firstly average some spectra (e.g., averaging 6 seconds spectra in this test work) that are close in time sequence (aim to improve signal-to-noise ratio). Based on this advantage, we could then set a reasonable threshold to remove the beam-combined RFI (see Figure 4). After removing the beam-combined RFI, there exist several strong RFI, indicating this strategy is effective. Those still existing strong RFI in Figure 4 could be occasional RFI coming into the receivers.

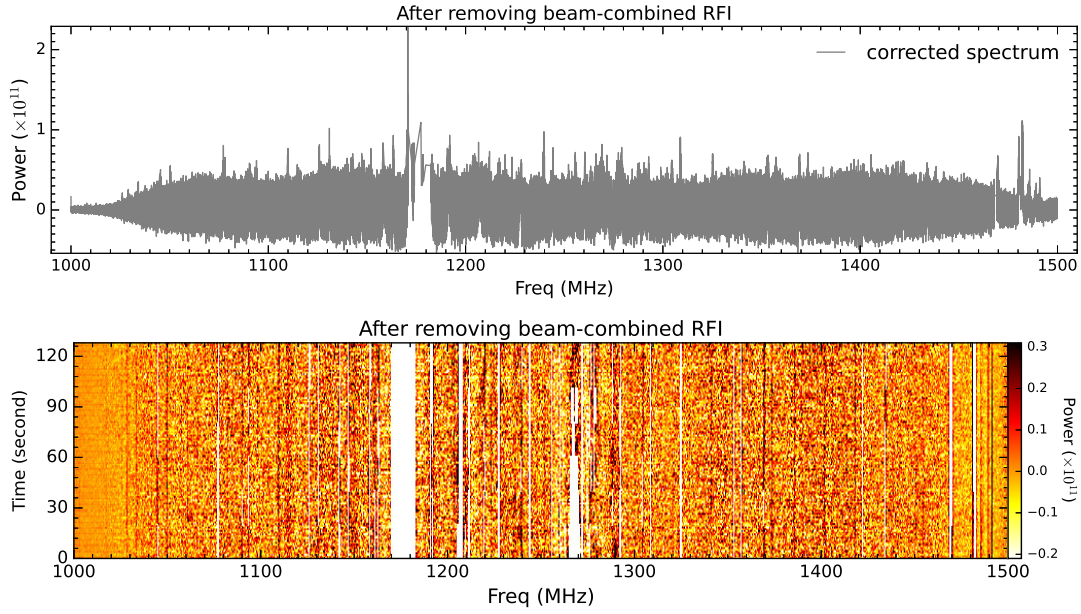


Fig. 4 Upper: A FAST spectrum (integration time: 1 second) after removing beam-combined RFI above a threshold of 4σ . Lower: A 128 seconds waterfall image after removing beam-combined RFI.

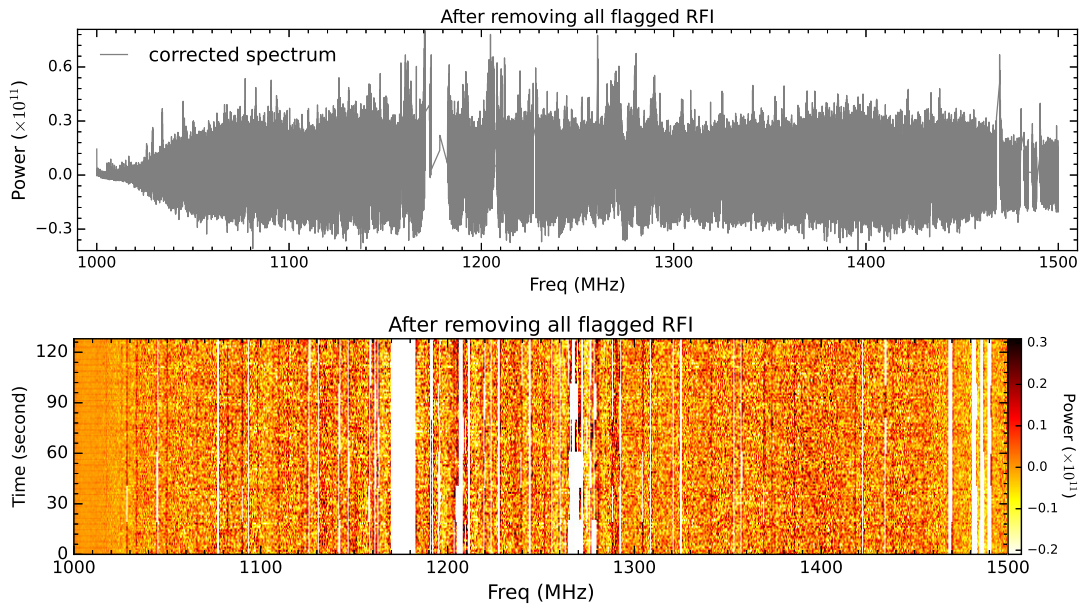


Fig. 5 Upper: A FAST spectrum (integration time: 1 second) after removing all the flagged RFI. Lower: A 128 seconds waterfall image after removing all the flagged RFI.

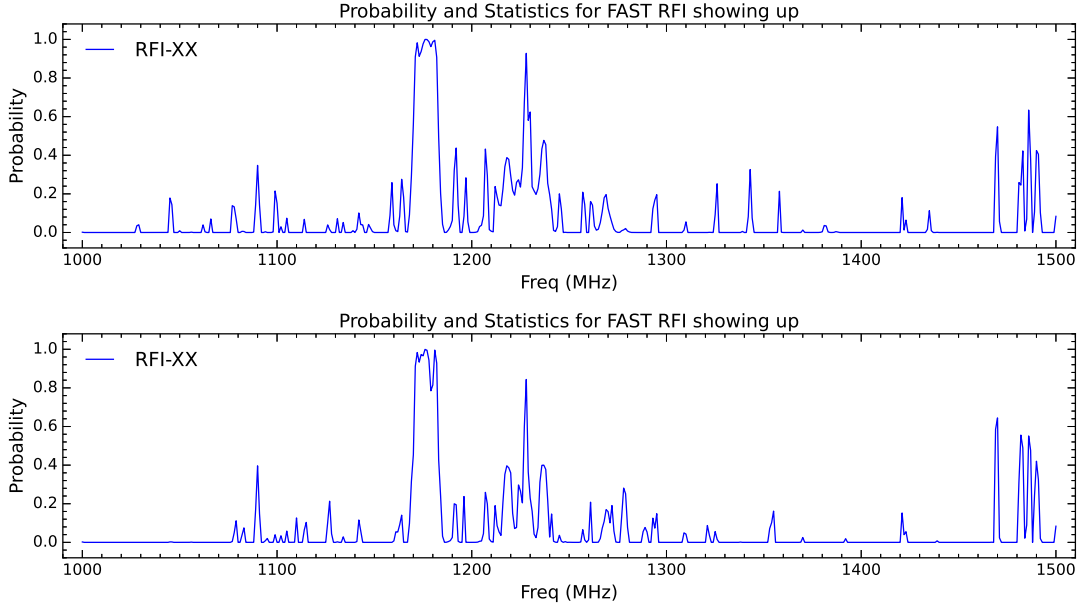


Fig. 6 Probabilities of polarized XX (upper panel) and YY (lower panel) RFI showing up in FAST spectral observations. The corresponding data are listed in Table 1.

3.2.5 Remove all the flagged RFI

The upper panel of Figure 5 shows a FAST spectrum after removing all the flagged RFI. We can see that those obvious RFI, compared with the spectrum in Figure 1, have been removed from the whole wideband. The 128 seconds waterfall image in the lower panel of Figure 5 show that the spectral data become flat already. However, there still exist several RFI, for example at 1170, 1210, 1260, and 1470 MHz. The existing RFI could be further flagged by improving the flagging threshold.

4 RFI STATISTICS

Based on the RFI flagging process, we found that there are indeed many RFI in the FAST spectral observation. We also found that some RFI are random and occasional, others are fixed at some frequencies. Since we already have a method to flag all the RFI above some threshold, it deserves to make a statistics for the probabilities of the RFI showing up in FAST spectral observations (see Figure 6 and Table 1). The statistical results would tell us which frequencies are relatively quiescent and which are noise. To do it, firstly we evenly split the 500 MHz wideband into 500 channels². Each channel will have a bandwidth of 1 MHz. With our RFI flagging procedure, we could find each RFI in every spectrum from long enough time observations. Then, we could compute the probability for each RFI showing up in each channel (1 MHz bandwidth) and each polarization (XX or YY).

From Figure 6, we found that the RFI with different polarizations (XX or YY) have obvious discrepancies at some frequencies. This further suggest that the terrestrial RFI are mostly polarized. In addition, the probabilities for the flagged RFI in most wideband are lower than 30%, but the RFI pollution is very serious, for example $P > 60\%$ at ~ 1175 , ~ 1225 , and ~ 1490 MHz. Even some RFI linewidths achieve to 20 MHz. For the convenience of query, Table 1 lists the detailed RFI frequencies with $P(XX) > 0$ or $P(YY) > 0$. Therefore, we should try to avoid using such frequencies in our spectral observations.

² Off course it can be easily splitted into more channels for statistical requirements.

Table 1 Probability for FAST RFI showing up.

Freq (MHz)	$P(XX)$ (%)	$P(YY)$ (%)	Freq (MHz)	$P(XX)$ (%)	$P(YY)$ (%)	Freq (MHz)	$P(XX)$ (%)	$P(YY)$ (%)	Freq (MHz)	$P(XX)$ (%)	$P(YY)$ (%)
1000.0	0.143	0.210	1162.0	0.454	5.349	1226.0	33.517	20.457	1325.0	9.291	5.583
1028.0	3.472	0.000	1163.0	8.507	9.187	1227.0	67.457	59.937	1326.0	25.219	1.568
1029.0	3.998	0.000	1164.0	27.554	14.082	1228.0	92.785	84.369	1334.0	0.013	0.000
1030.0	0.001	0.000	1165.0	18.304	0.033	1229.0	58.082	36.531	1335.0	0.039	0.000
1035.0	0.001	0.000	1166.0	0.438	0.065	1230.0	62.408	22.937	1336.0	0.015	0.000
1041.0	0.009	0.000	1167.0	0.207	0.059	1231.0	23.703	16.177	1338.0	0.001	0.143
1044.0	0.030	0.000	1168.0	9.164	9.817	1232.0	21.574	4.293	1339.0	0.559	0.000
1045.0	17.870	0.229	1169.0	29.198	31.602	1233.0	19.718	2.419	1342.0	8.222	0.019
1046.0	14.384	0.210	1170.0	56.057	45.323	1234.0	22.675	7.674	1343.0	32.612	0.000
1050.0	0.909	0.000	1171.0	90.995	91.264	1235.0	30.143	31.168	1344.0	7.538	0.000
1055.0	0.010	0.019	1172.0	98.240	98.325	1236.0	43.254	39.914	1353.0	0.000	7.170
1056.0	0.172	0.124	1173.0	91.219	93.310	1237.0	47.733	39.990	1354.0	0.000	10.201
1062.0	3.949	0.000	1174.0	93.716	97.294	1238.0	45.535	37.772	1355.0	0.000	16.183
1063.0	0.340	0.000	1175.0	97.652	96.616	1239.0	25.490	21.734	1356.0	0.000	0.004
1066.0	7.025	0.000	1176.0	99.994	99.943	1240.0	19.613	2.745	1358.0	21.339	0.000
1077.0	13.877	0.440	1177.0	99.946	99.943	1241.0	12.119	14.689	1359.0	0.128	0.000
1078.0	13.277	4.971	1178.0	98.823	94.369	1242.0	1.080	0.552	1369.0	0.000	0.087
1079.0	7.102	11.167	1179.0	96.233	78.490	1243.0	0.534	0.092	1370.0	1.267	2.514
1082.0	0.597	3.776	1180.0	98.760	81.511	1244.0	2.989	0.000	1371.0	0.034	0.000
1083.0	0.527	7.514	1181.0	99.550	99.580	1245.0	20.013	3.680	1374.0	0.006	0.000
1087.0	0.001	0.000	1182.0	90.731	92.803	1246.0	12.198	0.621	1378.0	0.014	0.000
1088.0	0.175	0.019	1183.0	49.366	42.725	1248.0	0.098	0.378	1379.0	0.082	0.000
1089.0	14.288	16.915	1184.0	20.156	23.925	1250.0	0.019	0.048	1380.0	0.360	0.000
1090.0	34.754	39.621	1185.0	4.221	3.177	1253.0	0.002	0.000	1381.0	3.618	0.000
1091.0	14.143	14.814	1186.0	0.001	0.001	1256.0	0.001	0.174	1382.0	3.421	0.000
1092.0	0.002	0.000	1187.0	0.085	0.079	1257.0	20.873	6.573	1383.0	0.287	0.000
1094.0	0.380	0.851	1188.0	1.318	0.402	1258.0	14.503	1.272	1384.0	0.024	0.000
1095.0	0.000	2.008	1189.0	3.107	0.928	1260.0	0.000	1.273	1385.0	0.001	0.000
1098.0	0.258	0.000	1190.0	6.258	2.533	1261.0	16.065	20.803	1386.0	0.059	0.000
1099.0	21.498	3.948	1191.0	32.163	19.982	1262.0	14.163	0.000	1387.0	0.447	0.000
1100.0	15.145	0.000	1192.0	43.751	19.465	1263.0	3.299	0.003	1388.0	0.215	0.000
1102.0	2.975	3.428	1193.0	14.159	0.554	1264.0	1.178	0.023	1390.0	0.003	0.000
1104.0	0.048	0.029	1194.0	0.029	0.000	1265.0	1.698	0.087	1391.0	0.008	0.010
1105.0	7.396	5.839	1195.0	0.000	0.003	1266.0	5.068	1.985	1392.0	0.010	1.912
1107.0	0.003	0.000	1196.0	8.429	23.746	1267.0	10.782	7.296	1407.0	0.003	0.001
1109.0	0.000	0.069	1197.0	28.312	0.039	1268.0	17.983	10.896	1408.0	0.000	0.003
1110.0	0.000	12.653	1198.0	5.545	0.000	1269.0	19.645	16.965	1419.0	0.001	0.000
1114.0	6.811	6.491	1200.0	0.001	0.000	1270.0	12.530	15.923	1421.0	18.049	15.229
1115.0	0.000	10.345	1201.0	0.017	0.000	1271.0	8.548	10.084	1422.0	1.254	3.958
1126.0	3.950	10.240	1202.0	0.112	0.025	1272.0	4.965	19.064	1423.0	6.416	5.545
1127.0	1.511	21.306	1203.0	0.421	0.117	1273.0	1.728	5.936	1434.0	1.615	0.000
1128.0	0.000	4.438	1204.0	3.047	0.551	1274.0	0.481	0.160	1435.0	11.290	0.000
1131.0	7.133	0.268	1205.0	3.749	0.699	1275.0	0.050	0.008	1436.0	0.930	0.000
1132.0	0.012	0.000	1206.0	8.596	4.522	1276.0	0.069	0.004	1439.0	0.094	0.793
1133.0	0.045	0.000	1207.0	43.214	25.901	1277.0	0.918	13.483	1467.0	0.019	0.076
1134.0	5.184	2.878	1208.0	29.480	19.853	1278.0	1.352	28.112	1469.0	39.290	58.519
1139.0	0.946	0.000	1209.0	1.490	1.722	1279.0	2.061	25.170	1470.0	54.728	64.453
1141.0	1.694	0.402	1210.0	0.652	0.384	1280.0	0.755	7.800	1471.0	5.699	2.355
1142.0	10.115	11.587	1211.0	0.341	0.117	1281.0	0.261	0.003	1481.0	25.887	31.245
1143.0	4.066	5.774	1212.0	23.797	19.013	1282.0	0.028	0.002	1482.0	24.526	55.554
1144.0	3.949	0.000	1213.0	18.643	8.653	1288.0	0.000	5.600	1483.0	42.237	48.887
1145.0	0.002	0.000	1214.0	14.206	5.451	1289.0	0.002	7.708	1484.0	0.770	2.162
1146.0	0.004	0.000	1215.0	13.847	3.581	1290.0	0.002	5.385	1485.0	6.967	8.968
1147.0	4.161	0.000	1216.0	22.372	20.602	1291.0	0.003	0.000	1486.0	63.388	55.108
1148.0	2.345	0.000	1217.0	34.063	35.231	1293.0	12.221	12.533	1487.0	38.149	47.658
1149.0	0.454	0.000	1218.0	38.774	39.655	1294.0	16.751	7.361	1489.0	10.593	24.222
1150.0	0.001	0.000	1219.0	37.876	38.623	1295.0	19.585	14.847	1490.0	42.428	42.020
1152.0	0.058	0.057	1220.0	29.375	35.979	1305.0	0.012	0.000	1491.0	40.519	32.398
1156.0	0.019	0.030	1221.0	21.758	15.035	1309.0	1.230	4.924	1492.0	10.330	1.968
1158.0	8.857	0.000	1222.0	19.321	7.189	1310.0	5.514	4.283	1500.0	8.365	8.365
1159.0	25.818	0.000	1223.0	25.995	7.704	1321.0	0.000	8.727			
1160.0	3.973	0.763	1224.0	27.294	29.728	1322.0	0.087	3.801			
1161.0	0.931	5.466	1225.0	23.510	26.614	1323.0	0.022	0.000			

Notes.

$P(XX)$ and $P(YY)$ are the probabilities of polarized XX and YY RFI showing up, respectively. The table only lists the RFI frequencies with $P(XX) > 0$ or $P(YY) > 0$.

5 SUMMARY AND FUTURE WORK

In FAST spectral observations, the RFI always influences the searching and analysis of the interesting astronomical objects. Mitigating the RFI becomes an essential procedure in the data reduction. Thus, we provide a method to mitigate the RFI in FAST spectral observation as follows.

Firstly, considering the FAST spectra have a very wide bandwidth (500 MHz), but its baseline is not flat enough. According to the characteristics of FAST spectra, we propose to use the ArPLS algorithm to do baseline fitting. The test results show that the ArPLS has a really good performance in the baseline correction of the FAST spectral data reduction.

Secondly, we flag the RFI in FAST spectra in four strategies, which are flagging extremely strong RFI, flagging long-lasting RFI, flagging polarized RFI, and flagging beam-combined RFI, respectively. The test results (see Figure 5) show that all the RFI above the preset threshold could be removed from the whole wideband efficiently.

Thirdly, we make a statistics for the probabilities of the RFI (including the polarized XX and YY) showing up in FAST spectral observations (see Figure 6 and Table 1). The statistical results could tell us which frequencies are relatively quiescent. With such statistical data, we could try to avoid using such frequencies in our spectral observations.

In future work, we will make a more detailed statistical work for the FAST RFI showing up. For example, when do the RFI always show up? Which sky region or telescope direction are more quiescent off the RFI? We will try to provide an efficient reference data for the FAST users.

ACKNOWLEDGEMENTS

FAST is a Chinese national mega-science facility, operated by the National Astronomical Observatories of Chinese Academy of Sciences (NAOC). C.-P.Z. acknowledges support by the NAOC Nebula Talents Program and the Cultivation Project for FAST Scientific Payoff and Research Achievement of CAMS-CAS.

References

- An, T., Chen, X., Mohan, P., & Lao, B. Q. 2017, *Acta Astronomica Sinica*, 58, 43
- Baan, W. A. 2011, in 2011 XXXth URSI General Assembly and Scientific Symposium, 1–2
- Baek, S.-J., Park, A., Ahn, Y.-J., & Choo, J. 2015, *The Analyst*, 140 1, 250
- Boonstra, A.-J. 2005, Radio frequency interference mitigation in radio astronomy, Ph.D. thesis, -
- Ford, J. M., & Buch, K. D. 2014, in 2014 IEEE Geoscience and Remote Sensing Symposium, 231–234
- Fridman, P. A., & Baan, W. A. 2001, *A&A*, 378, 327
- Han, J. L., Wang, C., Wang, P. F., et al. 2021, arXiv e-prints, arXiv:2105.08460
- Jiang, P., Tang, N.-Y., Hou, L.-G., et al. 2020, *Research in Astronomy and Astrophysics*, 20, 064
- Jiang, P., Yue, Y., Gan, H., et al. 2019, *Science China Physics, Mechanics, and Astronomy*, 62, 959502
- Kesteven, M. 2005, in *Proceedings. (ICASSP '05). IEEE International Conference on Acoustics, Speech, and Signal Processing, 2005.*, vol. 5, v/873–v/876 Vol. 5
- Nan, R., Li, D., Jin, C., et al. 2011, *International Journal of Modern Physics D*, 20, 989
- Zeng, Q., Chen, X., Li, X., et al. 2021, *MNRAS*, 500, 2969
- Zhang, C.-P., Xu, J.-L., Li, G.-X., et al. 2021a, arXiv e-prints, arXiv:2104.05272
- Zhang, H.-Y., Wu, M.-C., Yue, Y.-L., et al. 2020, *Research in Astronomy and Astrophysics*, 20, 075
- Zhang, T., Ren, J., Li, J., Nguyen, L. H., & Stoica, P. 2021b, arXiv e-prints, arXiv:2102.08987